Phototunable Response in Caged Polymer Brushes

Jiaxi Cui,[†] Thi-Huong Nguyen,[†,§] Marcelo Ceolín,[‡] Rüdiger Berger,[†] Omar Azzaroni,[†,‡] and Aránzazu del Campo[†,*]

[†]Max-Planck-Institut für Polymerforschung, Ackermannweg 10, 55128 Mainz, Germany

[‡]Instituto de Investigaciones Fisicoquímicas Teóricas y Aplicadas (INIFTA) CONICET, Universidad Nacional de La Plata, CC 16 Suc. 4 (1900) La Plata, Argentina

[§]Institute of Pharmacy and Biochemistry, Johannes Gutenberg University Mainz, Mainz 55128, Germany

ⓢ *Supporting Information*
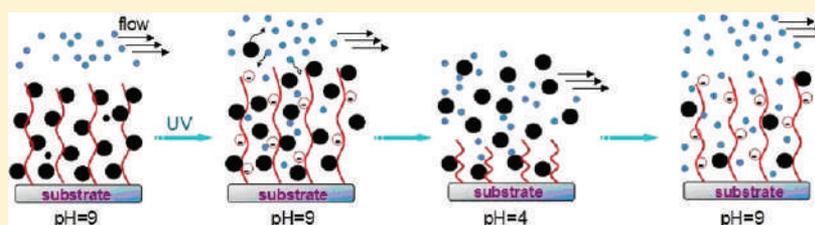
ABSTRACT: A light-responsive brush was obtained by surface-initiated ATRP of a methacrylate monomer containing ionizable −COOH side groups caged with the photoremovable group 4,5-dimethoxy-2-nitrobenzyl (NVOC). In the caged form, the polymer brush (PNVOCMA) is neutral and hydrophobic due to the presence of the aromatic chromophore. Upon irradiation the NVOC group is removed and a polyanion (polymethacrylic acid, PMAA) chain is generated. The charged brush can swell and collapse depending on the pH and the exposure dose (i.e., uncaging degree). The behavior and properties of the brush layer for different photoconversion degrees were studied. On the basis of quartz crystal microbalance measurements, a threshold of 50% uncaging was identified in order to achieve significant swelling and pH response of the brush. Between 50 and 80% the photoconversion the response of the brush could be light-modulated. For photoconversions >80% only small changes in the response were detectable. X-ray reflectivity (XRR) and scanning force microscopy allowed us to measure thickness, roughness and swelling of the brushes at intermediate photoconversions. Combined XRR and grazing-incidence small-angle scattering experiments evidenced a change in the internal structure of the brush upon exposure and indicated the occurrence of domain segregation as a consequence of the coexistence of hydrophobic and charged groups in the brush structure.

■ INTRODUCTION

The use of photolabile protecting groups ("cages") for photo-inducing changes in the macromolecular structure and resulting material properties has raised increasing interest in the past few years.[1] Light-triggered assembly and reorganization of caged block copolymers[2−4] and derived micelles,[5] disruption and swelling of nanoparticles containing drugs,[6] assembly and poly-merization of supramolecular polymers[7] and hydrogels,[8,9] or the generation of surface patterns[10] are recent examples that demonstrate the variety of effects that can be achieved by in-cluding photolabile units in the structure of the polymer chain (either directly in the main chain or on functional side groups). Photolabile polymer brushes containing caged ionizable side groups have also been recently realized.[11−16] Light exposure triggers the generation of charged units along the brush and induces a pH-dependent conformational change between the extended and collapsed states,[15,16] Wettability,[11,12,16] and permeability[15] changes on surfaces and interfacial architectures (membranes) have been demonstrated with these systems.

Most of the published studies on caged polymer systems con-centrate in the initial (caged) and final (fully uncaged) states and derived properties. However, light allows precise dosage and modulation of the photocleavage reaction and, therefore, the generation of well-defined intermediate chemical states with light-tunable properties. Minimum thresholds or saturation levels for the light-response have not been investigated. Miscibility and compatibility issues at the nanoscale between uncaged caged units along the polymer chain may also well arise at intermediate conversions. All these effects merit careful investigation and might lead to unexpected responses and application fields.

In this context, this article studies the evolution of the response and the internal structure of a photolabile polymer brush during the photolytic process. The light-responsive brush is obtained by surface-initiated ATRP of a methacrylate mono-mer containing ionizable −COOH side groups caged with the photoremovable group 4,5-dimethoxy-2-nitrobenzyl (NVOC). NVOC was selected as caging group because its alcohol is commercially available as precursor for the synthesis and its photochemical properties are well-known. In the caged form, the polymer brush (PNVOCMA) is neutral and hydrophobic

Scheme 1. Schematic of the Formation, Photolysis, and Swelling of Photosensitive Polymer Brushes
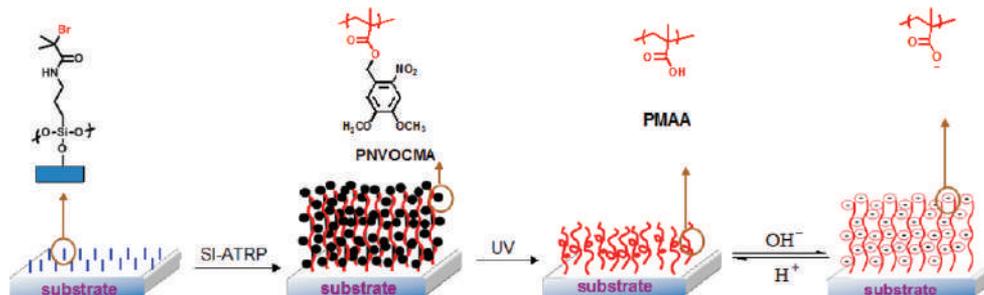
due to the presence of the aromatic chromophore (Scheme 1). Upon irradiation the NVOC group is removed and a polyanion (polymethacrylic acid, PMAA) chain is generated. The charged brush can swell and collapse depending on the pH and the degree of uncaging. The exposure dose will be controlled in order to investigate the behavior and properties of the brush layer for different photoconversion degrees. The minimum illumination threshold and the saturation levels for light-modulated swelling and pH response will be identified using a quartz crystal microbalance with dissipation (QCM-D). X-ray reflectivity (XRR) will be used to determine the changes in the film thickness and swelling of the brush for different uncaging ratios under different conditions. These data will be complemented by scanning force microscopy (SFM) data. Combined XRR and grazing-incidence small-angle scattering (GISAXS) experiments will provide information about the evolution of the mesostructural order in the brush.

■ EXPERIMENTAL SECTION

Materials and Methods. 2-Isocyanatoethyl methacrylate (98%, Aldrich), 4,5-dimethoxy-2-nitrobenzyl alcohol (98%, Alfa), (3-aminopropyl)triethoxysilane (APTS, 99%, Aldrich), 2-bromoisobutyryl bromide (BIB, 98%, Aldrich), N,N,N',N'',N''-pentamethyldiethylenetri-amine (PMDETA, 99%, Aldrich), copper(I) bromide (99.999%, Aldrich), and copper(II) bromide (99%, Aldrich), and poly(ethylene glycol) methyl ether (PEG, Aldrich, molecular weight ~550) were used as received. Methacrylic chloride (98%, Aldrich) was purified by distillation before use. All other reagents and solvents were used as obtained unless otherwise specified. Quartz slides (Suprasil 1) with a thickness of 1 mm were purchased from Heraeus Quarzglas (Hanau, Germany). Silicon wafers in (100) orientations were provided by Crystec (Berlin, Germany).

Solution ^{1}H and ^{13}C spectra were measured in CDCl$_3$ solution at 25 °C on Bruker Ultra Shield 250 MHz spectrometer. UV spectra were recorded on a Varian Cary 4000 UV−vis spectrometer (Varian Inc. Palo Alto, CA). Mass spectra were recorded on a Micromass Finnigan-MAT ZAB-HS mass spectrometer. Gel permeation chroma-tography (GPC) was performed with a polymer standard service (PSS) equipped with WinGPC. RI ERC 7512 (ERMA Inc.) and UV−Visible S-3702 (SOMA) were used as detectors. N,N-Dimethylforma-mide (DMF) was employed as eluent at a flow rate of 1.0 mL/min at 60 °C and columns SDV from PSS (100, 103, 104, and 106 Å porosity; 10 mm bead size; dimensions of 0.8 × 30 cm^2). GPC curves were calibrated against poly(methyl methacrylate) standards.

Synthesis. 4,5-Dimethoxy-2-nitrobenzyl methacrylate (NVOC-MA) was synthesized by reaction of 4,5-dimethoxy-2-nitrobenzyl alcohol and methacrylic chloride as previously reported[17] and purified via column chromatography (dichloromethane/ethyl acetate (10/1, v/v) as eluent) followed by recrystallization in ethanol before polymer-ization. PEG-based initiator (PEGBr) for performing ATRP in solu-tion was synthesized by the reaction of poly(ethylene glycol) methyl ether and BIB in the presence of triethylamine following the conditions reported in the literature.[16] Polymer brushes were prepared

by surface-initiated ATRP (SI-ATRP) on quartz or silicon wafers.[15,16] The substrates were first coated with the ATRP initiator (APTS + BIB), followed by immersion into a DMSO solution of the monomer, N,N,N',N'',N''-pentamethyldiethylenetriamine, CuBr, and CuBr$_2$, in a molar ratio of 100:3:1:0.1 under continuous stream of nitrogen and at 90 °C and free initiator PEGBr (0.04 mol % of monomer).[15,16]

Light-Exposure and Photocleavage. Irradiation experiments were carried out using a PolychromeV lamp (TILL Photonics GmbH, Grafelfing, Germany) at 365 nm (4.7 μW cm^{-2}). After irradiation, substrates were washed with CH$_2$Cl$_2$ and Milli-Q water to remove the photocleaved chromophore. For the patterning experiments, a mask with 5 × 5 μm quartz squares separated by 5 μm gold spacers was placed on the substrate during exposure.

Quartz Crystal Microbalance with Dissipation (QCM-D) Measure-ments. were carried out in a Q-Sense E1 system (Sweden). A silica-coated crystal was used (Q-Sense, Sweden). The crystal was excited at its fundamental frequency (5 MHz), and measurements of the frequency and dissipation change (Δf, ΔD) were performed at the first, third, fifth, seventh, ninth, and 13th overtones, corresponding to 5, 15, 25, 35, 45, and 55 MHz. A 100 mM KCl aqueous solution was used as flow medium, and the pH value was adjusted with either KOH or HCl aqueous solution. A window cell that allowed in situ light exposure was used for the experiments.

X-ray Reflectivity (XRR) and Grazing-Incidence Small-Angle X-ray Scattering (GISAXS) Measurements. were performed at the D10A-XRD2 beamline of Laboratório Nacional de Luz Síncrotron (LNLS) (Campinas, Brazil) (λ = 1.608 Å). The sample-to-detector distance was kept to 550 mm, the outgoing photons were detected using a PILATUS 100 K detector (DECTRIS AG, Switzerland). Sample temperature was kept to 20 °C and sample humidity was controlled using a home-built chamber.

Scanning Force Microscopy (SFM) Measurement. The SFM (NanoWizard, JPK, Berlin, Germany) was operated in contact mode at lowest possible normal forces to keep overlapping trace and retrace scan lines. Au back-side coated silicon nitride cantilevers with a nominal spring constant of 0.12 N/m (NP, Olympus, Japan) were used. Before measurement, the sample was rinsed with water and mounted on a glass slide by using a double side adhesive tape. Then, the glass slide was installed on the SFM sample holder and buffer solution (100 mM KCl aqueous solution, HCl was used to adjust the pH to 4) was injected in the liquid cell. The setup was left for 6 h for stabilizing conformation of polymer brushes and thermal equilibration before measurement. For imaging a scan speed of 0.3 Hz per line was used with a normal force of ~0.2 nN at a scan length of 30 μm. After a series of measurements at pH 4 the buffer was removed from the liquid cell by a syringe and the sample was thoroughly rinsed with 1 mL water. Subsequently, one milliliter of buffer (100 mM KCl aqueous solution, KOH was used to adjust the pH to 9) was injected in the liquid cell and the sample was left again for another 6 h before imaging. Then, a second series of imaging of the sample surface at the same position was recorded. During one measurement, the sample typically remained for 7 h at pH 9, 15 min in water for rinsing and 7 more hours at pH 4. The pH switching cycle was repeated three times. The images were processed and analyzed using Gwyddion software. An average of 20 line profiles at the center of each pattern was analyzed to determine the height difference between UV-irradiated
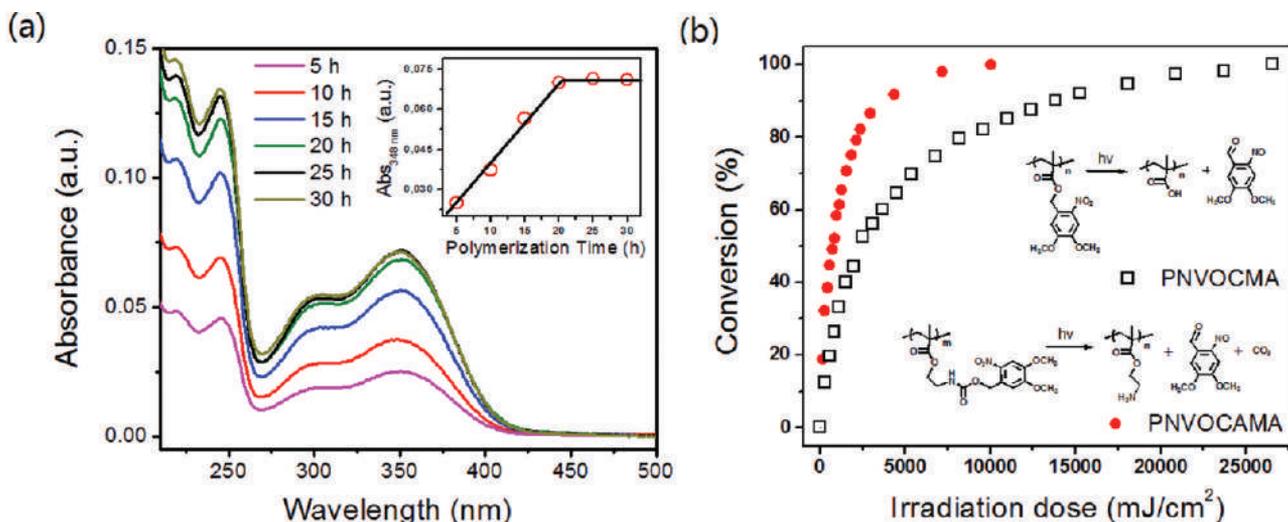
Figure 1. (a) UV spectra of PNVOCMA polymer brushes on quartz slides obtained with increasing polymerization times. The inset represents the linear increase in absorbance at 348 nm vs the polymerization time. (b) Conversion (%) for the photocleavage of PNVOCMA and PNVOCAMA brush at the surface upon irradiation at 365 nm. Data were calculated from the absorbance values at λ_{max} = 348 nm. Data of PNVOCAMA were extracted from ref 16.

and nonirradiated patterns. By comparing the height measured at the same position at pH 9 and pH 4, the swelling and deswelling of the polymer brushes at different pH was determined.

■ RESULTS AND DISCUSSION

Synthesis and Photochemical Properties of the Polymer Brush. The growth of the polymer brushes onto quartz substrates was followed by the increase in the UV absorbance. Figure 1 represents the UV−vis spectra of PNVOCMA brushes with increasing polymerization time. A linear increase in the absorbance was observed during the first 20 h of polymerization (inset in Figure 1), before polymer growth completely stopped. We hypothesized that the termination of the surface polymerization was due to the hydrolysis of the ester bond under our experimental conditions, rendering methacrylic acid that would poison the copper complex and stop chain growth.[18] ^{1}H NMR analysis of the polymerization reaction in solution showed the appearance of a signal at 4.78 ppm after 16 h reaction time that can be attributed to the methylene group of 4,5-dimethoxy-2-nitrobenzyl alcohol, confirming our hypothesis (Figure S1, Supporting Information). For this reason, we kept a polymerization time of 15 h for all substrates in order to obtain fully caged brushes.

Free initiator was added into the SI-ATRP solution and the obtained polymers in solution were isolated and characterized in order to estimate the molecular weight and distribution of the brushes.[16] The average molecular weight M_n was determined from the integrals of the ^{1}H NMR signals at 6.5−7.8 ppm for the aromatic proton and at 2.8−4.4 ppm for the methylene protons of the ethylene glycol chain (Figure S2, Supporting Information). The polydispersity index (PDI) was obtained by GPC. Values of M_n = 13300 g/mol and PDI = 1.48 were obtained after 15 h polymerization. Assuming that chains generated from free initiator in solution reach the same molecular weight as those from initiator at the surface,[19] the grafting density of the brush, Γ, can be estimated from the value of the degree of polymerization and the measured UV absorbance according to[20]

$$\Gamma = 1/2[A_\lambda \varepsilon_\lambda^{-1} n^{-1} N_A]$$

A_λ is the absorbance at a given wavelength, ε_λ is the molar extinction coefficient of the chromophore in solution at λ (ε_{348} = 6300 M^{-1} cm^{-1}), n is the average degree of polymerization and N_A is Avogadro's number. The factor $^1/_2$ refers to the fact that the quartz slides are modified on both sides. An average grafting density of 0.56 chains/nm^2 was obtained for PNVOCMA after 15 h polymerization.

Light exposure of quartz substrates modified with the polymer brushes cleaved the chromophore from the brush (Scheme 1) and the photolytic reaction was monitored by the decay of the UV absorbance of the substrates after exposure and a washing step (Figure S2, Supporting Information). Assuming that the detected absorbance is only associated with remaining chromophore on the brush, the conversion (%) of the photolytic reaction was calculated for the different exposure doses (Figure 1b). Following the photokinetic equation model for the special case of photolysis at surfaces,[21] a quantum yield (Φ_{365}) of 0.0071 was obtained for the photolysis of the surface attached chromophore. This value is close to the quantum yield reported for NVOC-caged phosphate esters in solution (0.003−0.009),[22] suggesting that the photolysis process and mechanism is similar in solution and on the surface. The quantum yield for the photolysis of nitrobenzyl derivatives is known to vary with the nature of the leaving group.[17,23] Figure 1b compares the conversion data of PNVOCMA (ester leaving group) with those of poly(2-[[(4,5-dimethoxy-2-nitrobenzoxy)-carbonyl]aminoethyl) methacrylate, PNVOCAMA (carbamate leaving group) that we recently published.[16] PNVOCAMA was photocleaved more effectively than PNVOCMA at a given irradiation dose (i.e., 50% of PNVOCMA and 75% of PNVOCAMA were photocleaved at 2800 mJ/cm^2) and the Φ_{365} of PNVOCAMA was 0.026, significantly higher than that of PNVOCMA.

The photolytic reaction was also reflected in a change in the contact angle of the brush layers. In caged state, the advancing, static, and receding contact angles were 74°, 68°, and 37° respectively. After exposure the layers turned more hydrophilic and contact angles of 66°, 63°, and <5° were measured.

QCM Studies for in Situ Monitoring the Phototunable Uncaging and Swelling of the Brush. Quartz crystal

microbalance (QCM) measurements were employed to follow the response of PNVOCMA brushes during light irradiation and pH cycling. The changes in the mass (associated with loss of the chromophore or uptake/release of water) were determined from the change in the resonant frequency (Δf). The ratio between the energy dissipated per cycle of oscillation and the total energy stored in the oscillating system was given by the D factor (ΔD).[24−26] We used a window-cell for the experiments that allowed direct illumination of the QCM crystal during measurement.

Figure 2a represents the Δf and ΔD of PNVOCMA under controlled light-exposure and pH changes. When the QCM
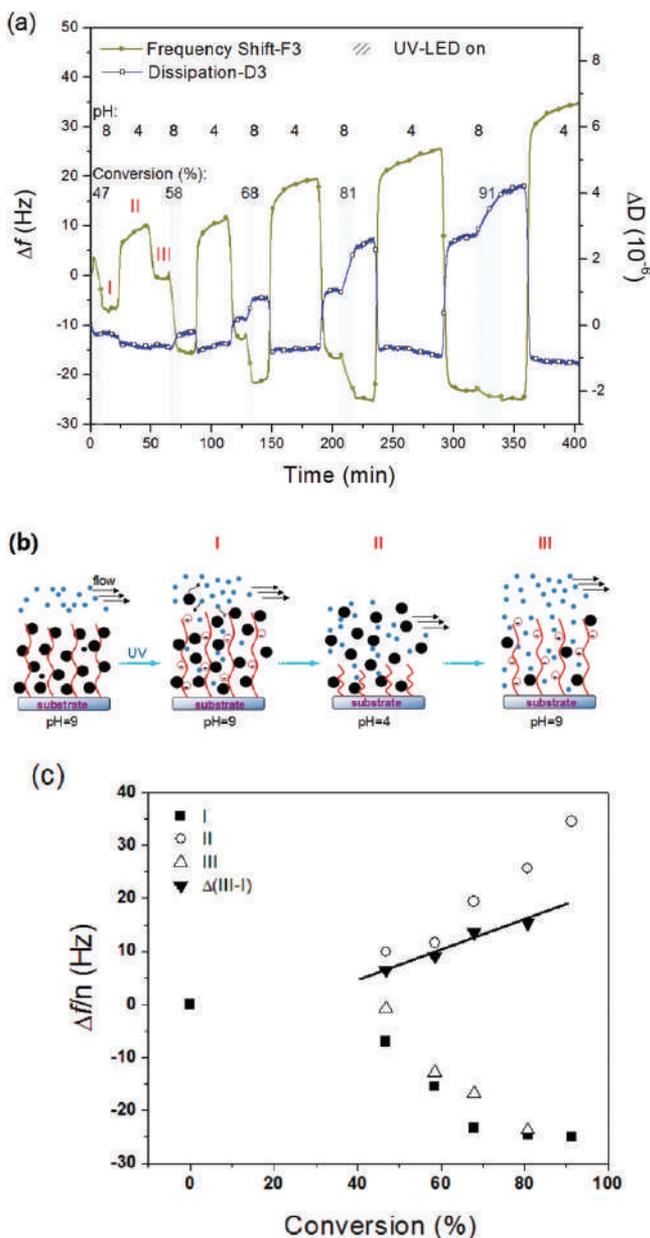

Figure 2. (a) Δf and ΔD of the third overtone of a SiO$_2$ QCM crystal coated with PNVOCMA brush under different conditions. (b) Representation of uncaging and swelling model. (c) $\Delta f/n(\Delta m)$ vs photolytic conversion plots.

crystal was modified with the caged brush (hydrophobic), it did not show any variation of Δf or ΔD at different pH, indicating no swelling of the brush in the buffer solutions (Figure S4,

Supporting Information). The crystal was then irradiated at pH 8 with a dose corresponding to 40% photoconversion. During exposure, the frequency continuously decreased, indicating an increase in mass of the surface layer. In parallel, an increase in the dissipation values, associated with an increase in the viscoelasticity of the surface layer, was observed. During exposure, the chromophore is cleaved from the brush and it is expected to diffuse out of the surface layer (mass loss). At the same time, the brush becomes hydrophilic and, therefore, may uptake water (i.e., increase in mass and viscoelasticity). In our case, the swelling of the now COOH functionalized chains, negatively charged at pH 8, was dominant for the mass change, as reflected by the decrease in Δf. When the irradiation was switched off, the frequency remained constant, demonstrating the possibility of light-modulated swelling of the caged brushes.[27] As the pH was changed to 4, a significant Δf increase indicated the loss of water and collapse of the polymer brush due to the protonation of the carboxyl group. When the pH was returned to 8, the polymer brush swelled again. However, Δf did not return to the same value, indicating that additional mass was lost during the collapsing state. We hypothesized that the mass loss corresponded to photolytic byproduct that remained embedded in the surface layer during irradiation at pH 8, but was squeezed out of the brush during collapse at pH 4. This means that hydration of the brush after uncaging happens at much faster rate than diffusion of the photoproducts out of the brush. A model representing the uncaging and swelling processes at the different conditions is shown in Figure 2b.

Further irradiation steps and pH cycles were performed up to full conversion and were followed in the QCM. Figure 2c displays the frequency shift values of the different steps vs the photolytic conversion. On the basis of our model, Δf values of steps I and III reflect the water uptake with increasing uncaging ratio (i.e., generation of carboxylate groups along the polymer brush) with and without chromophore, respectively. The frequency difference between steps I and III corresponds to the mass of lost chromophore and, in fact, it correlates linearly with the conversion values. Δf values from step II reflect the water uptake of the (partially) uncaged brush in the collapsed state. It is interesting to note that water uptake did not linearly correlate with the photolytic conversion. In fact, small changes in frequency were observed for uncaging ratios below 50%, but drastic changes were observed for higher conversions. This result suggests that a threshold of ca. 50% uncaged groups in the chain are required to swell the initially hydrophobic PNVOCMA brush.

Figure 3 shows the pH-sensitivity of the fully uncaged PNVOCMA brush, i.e. the PMAA brush.[28−31] At pH > 9, the brush is highly charged and adopts an extending conformation, adsorbing the highest amount of water.[32] By lowering the pH, the brush becomes less charged and more hydrophobic and chains collapse. This leads to shrinking of the brush and less water uptake. The highest change in swelling occurs from pH 6.0 to 7.0, as expected from reported works on homo-PMAA brushes.[33] At acidic pH the carboxyl group is protonated, the brush is neutral and the chains collapse. When the pH was returned from 4 to 9, the Δf reverts to the initial negative value, implying that the brush is stable and the swelling is reversible. These results confirm that the uncaging reaction renders fully functional PMAA brushes with the expected pH response.

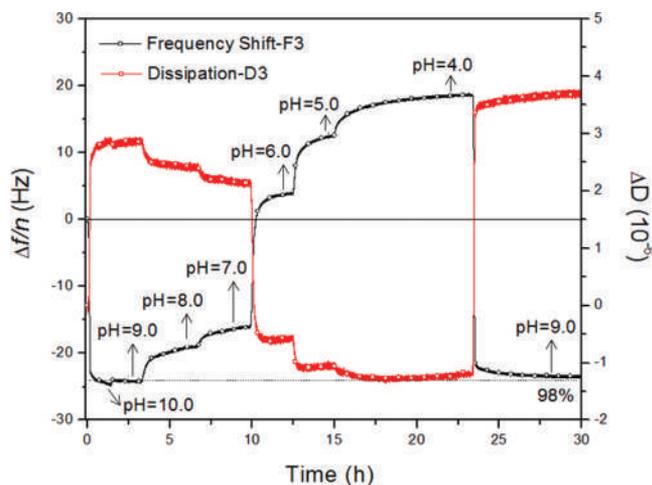**Evolution of the Thickness, Swelling, and Roughness of the Brush Layer upon Gradual Uncaging via XRR.**

Figure 3. Δf and ΔD of the third overtone of a SiO₂ QCM crystal coated with PNVOCMA brushes after full exposure and the variation with the pH.

XRR measurements were performed to determine the changes in the film thickness of the brush upon controlled exposure. Figure 4 shows the X-ray reflectometry spectra of PNVOCMA brushes upon 0% (caged brush), 30% and 100% photolytic conversion. Measurements were performed under low (0% RH) and high (>90% RH) relative humidity conditions. The film thickness, d, was calculated from the difference in the scattering vector q from maximum to maximum of the Kiessig fringes (the interval between fringes), according to $d = 2\pi/\Delta q$. The corresponding values are collected in Table 1. Caged PNVOCMA brushes had a thickness of 6.7 nm in dry conditions that increased to 7.0 nm at 90% humidity (swelling ~4%).

Table 1. Thickness of the Brush Layer and Roughness Values of PNVOCMA Brushes As Determined by X-ray Reflectivity under Different Environmental Conditions

photoconversion (%)	relative humidity 0%		relative humidity 90%	
	thickness (nm)	roughness (nm)	thickness (nm)	roughness (nm)
0	6.7	0.67	7.0	0.68
30	6.1	0.83	6.4	0.87
100	5.2	0.72	5.8	0.74

Upon partial (30%) and full (100%) photocleavage, the thicknesses of dry films decreased to 6.1 and 5.2 nm, respectively. The photolyzed films also swelled in humid conditions to a thickness of 6.4 and 5.8 nm (swelling ~5 and 10% respectively). As expected and in agreement with the QCM data, the fully exposed PNVOCMA brush, *i.e.*: PMAA brush, showed higher affinity for water than the caged or the partially photolyzed brush.

The stochastic roughness of the brush layer was calculated from the Gaussian decay of the amplitude of the Kiessig fringes superimposed to the typical q^{-4} decay of the scattering pattern.[34] Upon light exposure, the Kiessig oscillations at higher q-values became less pronounced. The suppression of Kiessig oscillations is a hint for an increase in the film roughness and suggests that the removal of the chromophore induces detectable structural changes in the polymer brush. Table 1 depicts

Figure 5. GISAXS patterns of PNVOCMA brushes with different photodeprotection degrees (PD): (top) 0%, (middle) 30%, and (bottom) 100%, obtained under dry conditions. The scattering vector q_y provides structural information on the lateral organization of polymer brush, whereas scattering features along q_z reveal changes normal to the surface of the thin film.
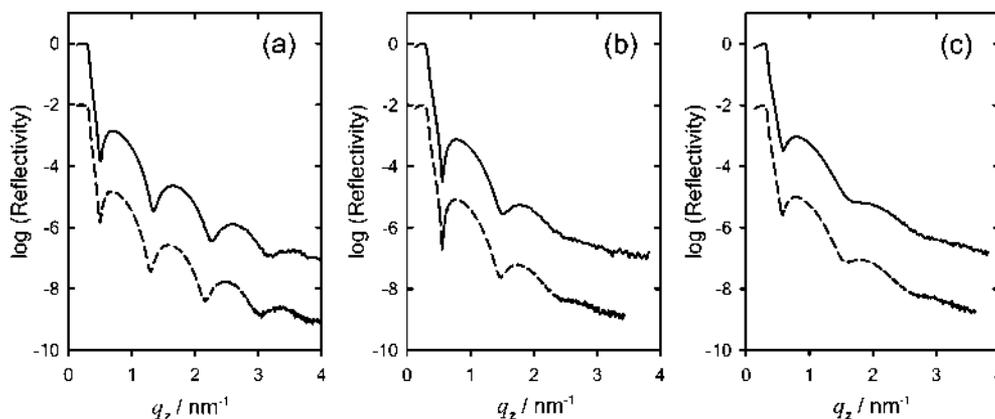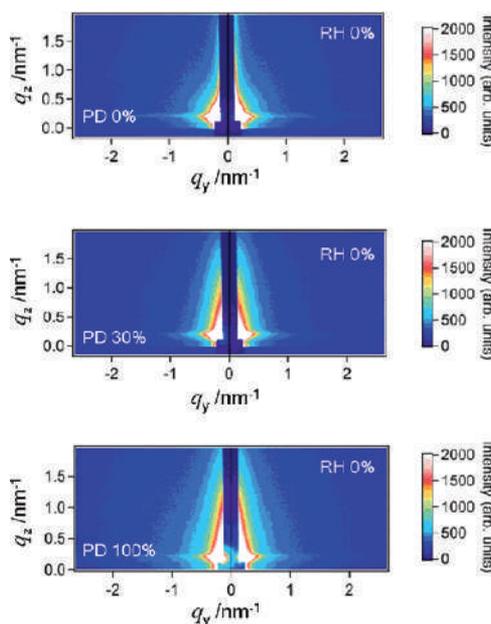

Figure 4. X-ray reflectivity data corresponding to PNVOCMA brushes after different degrees of photocleavage: (a) 0%, (b) 30%, and (c) 100%. Different traces correspond to experiments performed in dry (RH ~ 0%, dashed trace) and humid environments (RH ~ 90%, solid trace).
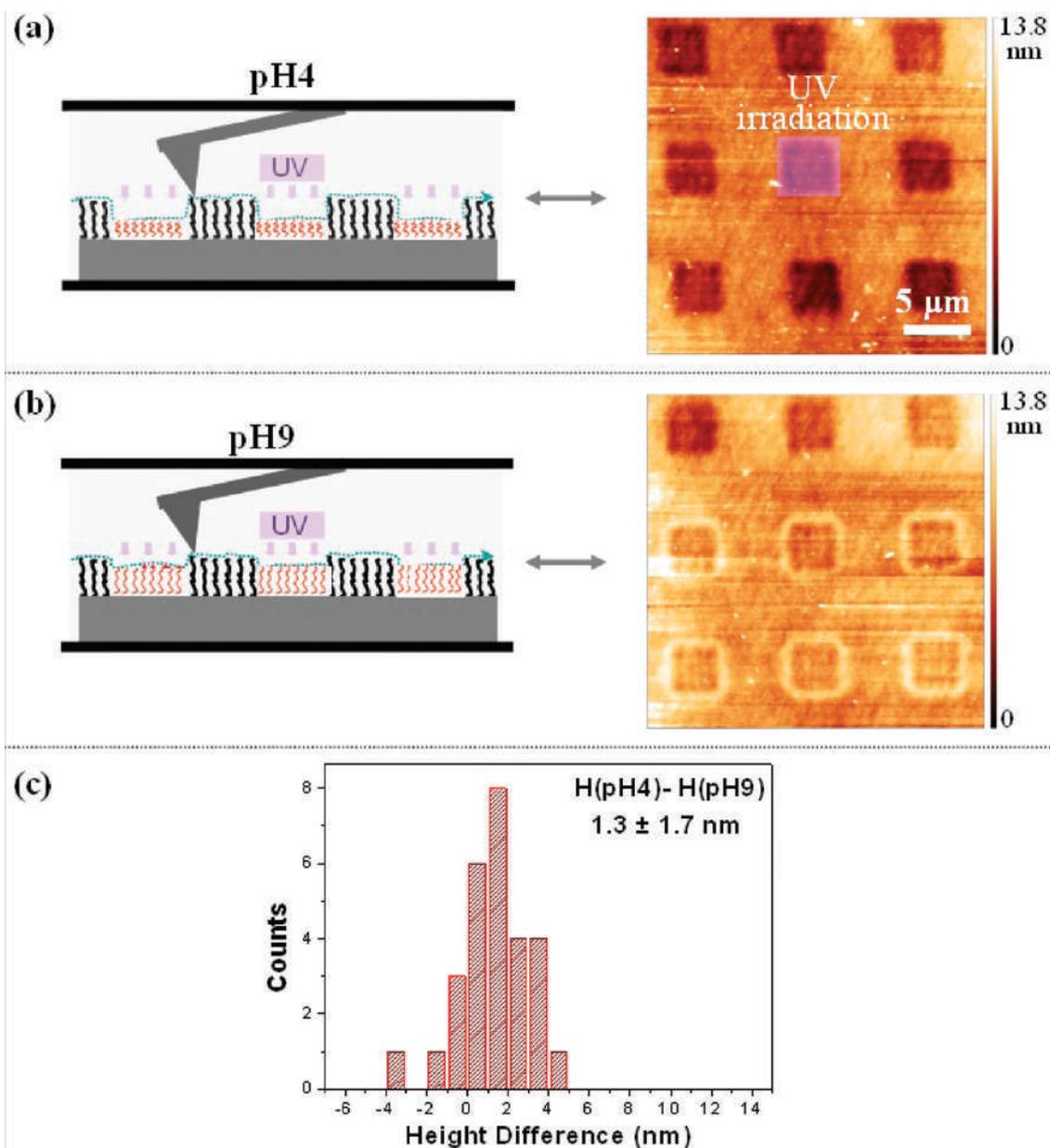
Figure 6. SFM contact mode imaging of masked-irradiated brush coated substrates at different pH. (a, b) Topography images taken at pH 4 (a) and pH 9 (b) with their corresponding sketches. (c) Histogram showing the distributions of different height collected from 3 measurements cycles and obtained from line profiles at ~30 different positions.

roughness values of caged and photolized brushes under different humidity conditions. We attribute the increase in roughness after partial photocleavage to a higher degree of heterogeneity in the brush layer due to the coexistence of hydrophilic and hydrophobic monomer units along the brushes. These could arrange into phase-segregated inner domains and lead to an increase in film roughness. The roughness in the fully exposed brush decreased again, reflecting the recovery of a brush with a homogeneous composition.

GISAXS Analysis of the Changes in the Internal Structure of the Brush upon Light Exposure. GISAXS measurements allowed us to investigate mesostructural order within the brush film.[35,36] The components of the scattering vector q_y and q_z enable discrimination between the scattering parallel and perpendicular to the sample surface and, therefore, they provide information about lateral and normal ordering within the thin film. Figure 5 and Figure S5 (Supporting Information) shows the GISAXS patterns of PNVOCMA brushes after controlled light exposure under dry and humid conditions. No significant changes in the GISAXS features between samples measured in humid or dry environments were observed. A comparative analysis of caged and irradiated samples revealed in both cases the absence of intensity maxima at finite scattering vectors which implies a broad distribution of domain sizes and/ or that domain−domain correlation does not play a significant contribution to the scattering, i.e. the scattering is dominated by the form factor of the domains and not from the in-plane structure factor of the film. For the condition $q_z \rightarrow 0$, we observe a similar intensity distribution on the left and on the right of the vertical symmetry for protected and unprotected brushes. Analysis of the out-of-plane scans (Guinier plots at $q_z = 0.1$ nm^{-1}) indicated the presence domains with in-plane diameters ca. 36 nm.

The scattering intensity in the direction perpendicular to the substrate (q_z) significantly changed upon light exposure, leading to a much smoother decay of scattering intensity toward larger q_z values (for $q_y \rightarrow 0$). The increase of scattering intensity at large q_z values suggests the creation of domains with smaller real-space dimensions stemming from the photocleavage process. In other words, the steeper decay of the intensity parallel to the sample surface rather than in the perpendicular direction means that the photogenerated hydrophilic domains distributed along the film thickness are flatter (or smaller in height) than the original "caged" hydrophobic domains.

Visualization of the Photoinduced Swelling on Photopatterned Brushes by SFM. Silica substrates modified with the PNVOCMA brushes were irradiated through a mask with 5 μm × 5 μm quartz squares separated by 5 μm gold spaces in order to generate surface patterns with caged and light-exposed brush areas. Scanning force microscopy (SFM) was used to probe the swelling and deswelling of the irradiated polymer brush at two different pH values (Figure 6). The SFM images recorded at pH 9 revealed the expected pattern geometry with 5 μm wide quadratic features. The light-exposed regions (that correspond to swollen PMAA brushes) appeared as recessed squares in the topography image. The depth of these areas (i.e., the height difference between caged brushes and uncaged brushes at pH 9) ranged from 1.5 to 5.0 nm depending on the exact position of the height measurement and the exposed area. This indicates that the thickness of the photocleaved brush layer after swelling was decreased compared to the original brush and, therefore, in agreement with the XRR measurements (Table 1). By changing the pH of the buffer in the liquid cell to 4, the difference between the height niveaus inside (PMAA) and outside (PNVOCMA) of the squares increased (in Figure 6 from b to a). A mean increase in the height difference of ~1.3 nm was estimated reflecting the higher swelling degree of the brush in the deprotonated state, as seen in the QCM experiments.

CONCLUSIONS

Polymer brush layers containing photolabile caged COOH lateral groups have allowed us to build surfaces with a light-modulated response to humidity and pH. The cleavage of the chromophore from the brush layer upon exposure occurs with similar photophysical parameters and yield than in solution. The consequent generation of ionizable groups renders a more hydrophilic brush layer able to swell up to 10% after full deprotection. The diffusion of the chromophore out of the brush layer is slow and can be accelerated by collapsing the brush at acidic pH. A threshold of 50% uncaging was necessary in order to achieve significant swelling and pH response of the brush. Between 50 and 80% photoconversion, the response of the brush could be light-modulated. For photoconversions >80%, only small changes in the response were detectable.

The internal structure of the brush layer was changed upon light exposure. This was reflected in an increase in the surface roughness at intermediate conversions, where hydrophilic and hydrophobic groups are forced to coexist in the brush structure. We interpret these results as an indication for domain segregation.

ASSOCIATED CONTENT

Ⓢ Supporting Information

^{1}H NMR of polymers, UV−vis spectra, Δf and ΔD plots, and QCM-D image. This material is available free of charge via the Internet at http://pubs.acs.org/.

AUTHOR INFORMATION

Corresponding Author

*Telephone: +49 (0)6131 379563. Fax: +49 (0)6131 379271. E-mail: delcampo@mpip-mainz.mpg.de.

Notes

The authors declare no competing financial interest.

REFERENCES

(1) Zhao, H.; Sterner, E. S.; Bryan Coughlin, E.; Theato, P. *Macromolecules* **2012**, DOI: 10.1021/ma201924h.

(2) Schumers, J. M.; Bertrand, O.; Fustin, C. A.; Gohy, J. F. *J. Polym. Sci., Part A: Polym. Chem.* **2012**, *50* (3), 599−608.

(3) Schumers, J. M.; Fustin, C. A.; Gohy, J. F. *Macromol. Rapid Commun.* **2010**, *31* (18), 1588−1607.

(4) Schumers, J. M.; Gohy, J. F.; Fustin, C. A. *Polym. Chem.* **2010**, *1* (2), 161−163.

(5) Bertrand, O.; Schumers, J. M.; Kuppan, C.; Marchand-Brynaert, J.; Fustin, C. A.; Gohy, J. F. *Soft Matter* **2011**, *7* (15), 6891−6896.

(6) Klinger, D.; Landfester, K. *Macromolecules* **2011**, *44* (24), 9758−9772.

(7) Foster, E. J.; Berda, E. B.; Meijer, E. W. *J. Am. Chem. Soc.* **2009**, *131* (20), 6964−6966.

(8) Peng, K.; Tomatsu, I.; van den Broek, B.; Cui, C.; Korobko, A. V.; van Noort, J.; Meijer, A. H.; Spaink, H. P.; Kros, A. *Soft Matter* **2011**, *7* (10), 4881−4887.

(9) Kloxin, A. M.; Kasko, A. M.; Salinas, C. N.; Anseth, K. S. *Science* **2009**, *324* (5923), 59−63.

(10) Shafiq, Z.; Cui, J.; Pastor-Pérez, L.; San Miguel, V.; Gropeanu, R. A.; Serrano, C.; del Campo, A. *Angew. Chem., Int. Ed.* **2012**, inpress.

(11) Brown, A. A.; Azzaroni, O.; Fidalgo, L. M.; Huck, W. T. S. *Soft Matter* **2009**, *5*, 2738−2745.

(12) Brown, A. A.; Azzaroni, O.; Huck, W. T. S. *Langmuir* **2009**, *25*, 1744−1749.

(13) Fries, K.; Samanta, S.; Orski, S.; Locklin, J. *Chem. Commun.* **2008**, *47*, 6288−6290.

(14) Samanta, S.; Locklin, J. *Langmuir* **2008**, *24* (17), 9558−9565.

(15) Brunsen, A.; Cui, J.; Ceolín, M.; del Campo, A.; Soler-Illia, G. J. A. A.; Azzaroni, O. *Chem. Commun.* **2012**, *48*, 1422−1424.

(16) Cui, J.; Azzaroni, O.; Del Campo, A. *Macromol. Rapid Commun.* **2011**, *32* (21), 1699−1703.

(17) Brown, A. A.; Azzaroni, O.; Huck, W. T. S. *Langmuir* **2009**, *25* (3), 1744−1749.

(18) Matyjaszewski, K.; Patten, T. E.; Xia, J. *J. Am. Chem. Soc.* **1997**, *119* (4), 674−680.

(19) Ohno, K.; Kayama, Y.; Ladmiral, V.; Fukuda, T.; Tsujii, Y. *Macromolecules* **2010**, *43* (13), 5569−5574.

(20) Stegmaier, P.; Alonso, J. M.; del Campo, A. *Langmuir* **2008**, *24* (20), 11872−11879.

(21) Wöll, D.; Walbert, S.; Stengele, K.-P.; Albert, T. J.; Richmond, T.; Norton, J.; Singer, M.; Green, R. D.; Pfleiderer, W.; Steiner, U. E. *Helv. Chim. Acta* **2004**, *87* (1), 28−45.

(22) Goeldner, M.; Givens, R. *Dynamic Studies in Biology: Phototriggers, Photoswitches and Caged Biomolecules*; Wiley-VCH: Weinheim, Germany, 2005; p 159.

(23) Cameron, J. F.; Frechet, J. M. J. *J. Am. Chem. Soc.* **1991**, *113* (11), 4303−4313.

(24) Cheng, N.; Azzaroni, O.; Moya, S.; Huck, W. T. S. *Macromol. Rapid Commun.* **2006**, *27* (19), 1632−1636.

(25) Moya, S. E.; Brown, A. A.; Azzaroni, O.; Huck, W. T. S. *Macromol. Rapid Commun.* **2005**, *26* (14), 1117−1121.

(26) Notley, S. M.; Eriksson, M.; Wågberg, L. *J. Colloid Interface Sci.* **2005**, *292* (1), 29−37.

(27) Konradi, R.; Ruehe, J. *Macromolecules* **2005**, *38* (14), 6140−6151.

(28) Liu, G.; Zhang, G. *J. Phys. Chem. B* **2008**, *112* (33), 10137−10141.

(29) Santonicola, M. G.; de Groot, G. W.; Memesa, M.; Meszyńska, A.; Vancso, , G. J. *Langmuir* **2010**, *26* (22), 17513−17519.

(30) Rahane, S. B.; Floyd, J. A.; Metters, A. T.; Kilbey, S. M. II. *Adv. Funct. Mater.* **2008**, *18* (8), 1232−1240.

(31) Patil, V.; Malvankar, R. B.; Sastry, M. *Langmuir* **1999**, *15* (23), 8197−8206.

(32) Moya, S.; Azzaroni, O.; Farhan, T.; Osborne, V. L.; Huck, W. T. S. *Angew. Chem., Int. Ed.* **2005**, *44* (29), 4578−4581.

(33) Dong, R.; Lindau, M.; Ober, C. K. *Langmuir* **2009**, *25* (8), 4774−4779.

(34) Tolan, M. *X-Ray Scattering From Soft-Matter Thin Films*; Springer-Verlag: Heidelberg, Germany, 1999.

(35) Lazzari, R. *Lect. Notes Phys.* **2009**, *770*, 283−342.

(36) Buschbaum, P. In *Polymer Surfaces and Interfaces Characterization, Modification and Applications*; Stamm, M., Ed.; Springer-Verlag: Heidelberg, Germany, 2008; Chapter 2, pp 17−46.